Combustion and Flame 176 (2017) 554–566

Contents lists available at ScienceDirect

Combustion and Flame

journal homepage: www.elsevier.com/locate/combustflame

Physical and chemical characteristics of flue-gas particles in a large pulverized fuel-fired power plant boiler during co-combustion of coal and wood pellets

Fanni Mylläri[a], Panu Karjalainen[a], Raili Taipale[b], Pami Aalto[c], Anna Häyrinen[d], Jani Rautiainen[d], Liisa Pirjola[e], Risto Hillamo[f], Jorma Keskinen[a], Topi Rönkkö[a,*]

[a] Aerosol Physics Laboratory, Department of Physics, Tampere University of Technology, P.O. Box 692, FI-33101 Tampere, Finland
[b] VTT Technical Research Centre of Finland, P.O. Box 1603, FI-40101 Jyväskylä, Finland
[c] School of Management/Politics, University of Tampere, FI-33101 Tampere, Finland
[d] Helen Oy, Helen, FI-00090 Helsinki, Finland
[e] Department of Technology, Metropolia University of Applied Sciences, FI-00180 Helsinki, Finland
[f] Atmospheric Composition Research, Finnish Meteorological Institute, FI-00560 Helsinki, Finland

ARTICLE INFO

Article history:
Received 5 August 2016
Revised 13 September 2016
Accepted 29 October 2016
Available online 10 December 2016

Keywords:
Biomass combustion
High temperature aerosol
Total particle number concentration
Particle number size distribution
Pulverized fuel
Coal

ABSTRACT

Fossil fuel combustion should be decreased in future years in order to lower the CO_2 emissions of energy production. The reduction can be achieved by increasing the amount of CO_2-neutral fuels in energy production. Here 6–13% of coal was substituted with industrial or roasted pellets in a pulverized fuel-fired power plant without making any changes to fuel grinding or low-NO_x burners. The effect of pellet addition for the flue gas particles was studied with direct sampling from the boiler super heater area. Based on primary dilution ratio tests, transmission electron microscope images, and the natural electric charge of the particles, it was observed that particles in the flue gas are spherical and have been formed in the boiler at high temperatures. The pellet addition lowered the total particle number concentrations with all of the studied pellet–coal mixtures in comparison to the coal combustion. The 10.5% industrial pellet addition caused a second mode in the particle number size distribution. In addition, based on the chemical analysis of the collected size-fractioned particle samples, results indicated that the pellet addition did not increase the corrosion risk of the boiler. However, the changes in the particle number size distribution and total particle number concentration can affect the operation of electrostatic precipitators and flue gas cleaning.

1. Introduction

Climate change has caused a global need to reduce CO_2 emissions. These emission reductions are driven mainly by local political decisions [1,2], but larger scale political actions also exist. In principle, smaller CO_2 emissions can be achieved by reducing the usage of fossil fuels in traffic, residential needs, and in power generation. This can take place by reducing the energy consumption or by substituting fossil fuels with renewable fuels (e.g., biofuels, solar and wind power). One likely cost effective possibility in these actions is to utilize existing coal-fired power plant infrastructures and substitute the coal used in those with biomass. However, decreased CO_2 emissions and the addition of biomass can change the emission of other harmful pollutants and also increase the corrosion risks for the power plant boilers. Biomass-based fuels have a different chemical composition than fossil fuels such as coal [3]. Biomass fuels typically contain more alkali metals and chlorides [3,4], which can, in the combustion process, be vaporized into the flue gas [5]. For instance, alkali chlorides are found to be harmful for the power plant boiler materials [6]. After the combustion process, corrosion-causing elements can exist in the vapour or particle phase [7], depending on the temperature and concentrations [8]. For instance, a change in the boiler temperature profile affects the deposition locations of the alkali chloride [8]. In principle, the amount of alkali chlorides in the particle phase can be determined when the particle size distribution and chemical composition of the particles are studied simultaneously.

In addition to the temperature profile existing in the boiler and the chemical composition of the fuel, the fuel grain size also has

* Corresponding author.
E-mail address: topi.ronkko@tut.fi (T. Rönkkö).

http://dx.doi.org/10.1016/j.combustflame.2016.10.027
0010-2180/

an effect on the combustion process and the slagging and fouling of the super heater surfaces. The fuel grain size affects the particle size distribution after combustion in the flue gas. Ninomiya et al. [9] have studied the effect of coal grain size in terms of particle mass (PM) emission. They discovered that <63 µm coal particles produce bimodal PM distribution, with mode means of 500 nm and 4 µm. They also found that there is a small mode around 130 nm, which consisted of alkali metals, heavy metals and their sulphate, chloride and phosphate salts. The flue gas is steered to flue gas ducts and released in to atmosphere with or without some flue gas cleaning. Particle properties such as size, chemical composition, and the electric charge carried by particles affect the flue gas cleaning efficiency [10,11].

In general, the flue-gas changes in large power plant boilers can affect, for example, the corrosion of the super heater area and other parts of the flue-gas system, the flue-gas cleaning systems and, finally, the emissions of power plants. These effects depend on the characteristics of aerosol generated in the combustion process. The emissions of particles from combustion plants and other sources are governed by the Convention on Long-Range Transboundary Air Pollution of the United Nations Economic Committee for Europe. The 2012 amendments to the Convention include national emission reduction commitments by 2020 and beyond. The limit values for SO_2, NO_x, ammonia, volatile organic compounds and particulate matter (i.e., with a diameter equal to or less than 10 µm), including black carbon, are separately defined for coal and biomass with no mention of co-combustion [12]. In addition to the EU Member States, Canada, the United States, Russia and several countries of Southern and Eastern Europe, the Caucasus and Central Asia are also expected to sign the amendments. In its related legislation, the European Union also separates the emissions from coal and biomass without any mention of prospects of co-combustion [13–15].

However, the partial substitution of coal by biomass and subsequent co-combustion is one of the pathways identified in the European Industrial Bioenergy Initiative (EIBI) of the European Commission and the EU Member States. The EIBI pays attention to local variation in the available biomass feedstock options and suggests "a pragmatic approach to select the most promising options, based on transparent criteria reflecting a set of key economic, environmental and social performances expected" [16]. The European Commission deems co-combustion of biomass and coal to be "the most cost-effective option for electricity production". Addition of biomass up to 10% share of total power output has been successfully demonstrated and the technology is commercially available. This technology makes use of existing plant infrastructure and requires only limited investments in biomass pre-treatment and feed-in systems [17]. However, "feeding, fouling and ash disposal pose technical challenges that reduce reliability and lifetime of coal plants. Higher co-firing mix will require more sophisticated boiler design, process control and fuel handling and control systems" [18]. The European Commission is hesitant towards to establish a specific policy for the co-combustion of biomass and coal. It notes that the incentives of the utilities running relevant combustion plants are national support schemes and/or the emission ceiling of the emissions trading scheme (ETS). Therefore setting a policy for co-combustion installations without similar measures for coal-combustion plants might lead to decreased use of biomass and hence, by implication, higher emissions [19].

In the United States, short tests of co-combustion have been conducted since the 1990s. The Energy Information Administration expects co-combustion to be up to 20 times more prevalent by 2024 than it was in 2010 [20]. Federal-level research into the heating qualities of different biomass contents and emissions continues [21]. The 2014 Clean Power Plan offered by President Obama and the Environmental Protection Agency mentions that, in co-combustion, the "use of some kinds of biomass has the potential to offer a wide range of environmental benefits, including carbon benefits", and that "[I]ncreasing renewable energy (RE) use will also continue to lower other air pollutants (e.g., fine particles, ground-level ozone, etc.)" [22]. While federal level regulation is debated, individual states can use renewable energy standards (RES) to incentivize power plant operators for co-combustion [20]. However, by 2012, only 3% RPS-motivated renewable energy capacity additions came from biomass [23]. With regard to co-combustion, plant operators hesitate over the costs of acquiring and transporting the biomass, as well as the long-term effects on process equipment [20].

In this article, flue-gas aerosol from a large scale pulverized coal-fired power plant boiler is investigated. The power plant combusted various mixtures of coal and two types of wood pellet. Special attention is paid to the particle number size distributions, total particle number concentration and chemical composition of particles in the diluted flue-gas sample taken from the boiler super heater area. In addition, the effects of wood pellets on the concentrations of gaseous species and particulate matter (PM) in the flue gas are shown. The aim is to understand the effect of co-combustion of wood pellets and coal on flue-gas aerosol formation and characteristics.

2. Experimental

2.1. Power plant

The power plant where the experiments of this study occurred is situated in Helsinki, Finland. In the power plant, there are two separate boilers, both equipped with flue gas cleaning systems that include electrostatic precipitators, semi-dry desulphurization, and fabric filters, in the given order after the boiler. Boilers (363 MW_{th}) are equipped with a reheater and utilizes the natural circulation of flue gas. Boilers are equipped with 12 low-NO_x technology burners (Tampella/Babcock-Hitachi HTNR low NO_x) that are at the front wall. The combustion air and at the same time the carrier air for the pulverized fuel is preheated up to 350 °C before the boiler and grinders. Main operation principle of low-NO_x burners is air staging with secondary and tertiary air, which lowers the combustion temperature to the level of around 1100 °C. Air staging decreases NO_x formation. The power plant boiler has originally been designed to combust pulverized coal that is fed to the boiler after being ground in ball ring grinders.

2.2. Fuel properties

In this study, some of the measurements were made with 100% Russian coal and some with mixtures of coal and pellets. In the latter case, coal was substituted with 6–13% (of the boiler thermal power) wood pellets; roasted pellets or industrial pellets (see experimental matrix in Table 1). Roasted pellet is torrefactioned wood pellet, also known as black pellet, steamed pellet, torrefactioned pellet and bio coal, manufactured from wood pellets by heat treatment at approximately 300 °C.

Industrial pellet (wood pellet of industrial quality) fulfils the standard EN 14961-1 requirements having lower quality than domestic quality wood pellets. Industrial pellet can include, for example, bark, which does not exist in higher quality wood pellets. Normally, wood for industrial pellets is gained by grinding stem wood or logs to powder and, after drying, by pressing the powder to pellets. Due to the preparation principle of industrial pellets, it is more brittle than domestic pellets and it contains more ash components.

Table 1
Experimental matrix. Coal was combusted during the nights and for that reason the "c" test took only 2 h. Note that there is a lower load in "c+rp7.6%" situation. The deviations we mainly caused by instability of the pellet feeding system.

Label	$Power_{coal}$	$Power_{pellet}$	Portion of pellet from fuel power (%)	DLPI sampling time	Duration of co-firing test
c+rp6.8%	301.6–322.2	5.2–33	1.6–9.9	2 h	3 h
c+rp7.6%	246.3–248.7	19.0–21.9	7.1–8.2	2 h 30 min	5 h
c+rp9.8%	294.7–320.3	15.7–44.1	4.7–13	2 h 10 min	5 h
c+rp13.1%	287.3–318.5	34.9–47.5	9.9–14.2	2 h	3 h
c+ip6.6%	299.2–312.9	12.8–31.8	3.9–9.6	2 h	5 h
c+ip10.5%	297.9–302.7	28.3–36.8	8.5–11.0	1 h 40 min	4 h
c	328.0–335.7	0	0	1 h 40 min	2 h

The coal is stored inside the power plant building in four intermediate storages, "day silos". From the intermediate storages the coal is divided to a belt conveyor which carries the coal to the grinders. Below each belt conveyor there is a grinder, which pulverizes the coal. The pellet is added to the grinder by a separate feeding system. The pulverization is performed with ball ring grinders (9 rolling balls). The pulverized fuel is blown into three burners together with the combustion air. Over each grinder there is a sieve which returns the largest particles back to the grinder. The fuel mixture was grinded simultaneously in two of the four grinders and thus in total 6 burners were combusting wood–pellet coal mixtures. When pulverizing coal the mean fuel particle size was 47–62 µm (58–69% was below 74 µm and 100% was <600 µm). For "c+rp" the mean fuel particle size was 56–90 µm (32–74% was below 74 µm and 87–100% was <600 µm), whereas for the "c+ip" the mean fuel particle size was 54–174 µm (28–59% was below 74 µm and 79–99% was <600 µm). These numbers show that the wood pellet substitution changes the pulverized fuel by increasing the fuel particle diameter.

Pellet and coal properties are listed in Table 2. Table 2 shows that the pellets had lower water and ash content in contrast to the coal. Also, the sulphur content and chloride contents were significantly lower in the pellets than the coal. Instead, the oxygen and volatile content were higher in the pellets than in the coal. It is notable, that the sum of alkali metals (K and Na) was higher in coal than in the pellets, which means that actually the pellet addition diluted the alkali concentration in the boiler. The heating value of coal was higher than the heating value of pellets.

2.3. Measurement setup and analytical methods

The measurement setup used is shown in Fig. 1. All the measurements with pure coal and coal–pellet mixtures were made from the same boiler unit. In these measurements, the flue-gas sample was taken from the boiler super heater area where the temperature ranges from 900 to 1000 °C. Due to the temperature variations and turbulence in the boiler, the flue-gas sampling was not designed to be isokinetic. This can affect representativeness of absolute concentration values measured for large particles, but not to the relative concentrations between the studied fuel-mixtures. Primary dilution of the sample was performed with a porous tube-type diluter using nitrogen (200 °C) as diluting gas, similar to the one in [24]. Due to the hot flue gas condition, the outer shell of the dilution probe was cooled with pressurized air flow, whereas the inner shell was heated to prevent the condensation of the gaseous components. Secondary dilution was performed with an ejector diluter (Dekati Ltd.), using nitrogen as a diluting gas, with a dilution ratio of 2.83. The primary dilution ratio was calculated based on CO_2 and H_2O measurements. In most of the measurements, the primary dilution ratios were between 6.0 and 8.3. The primary dilution ratio was chosen so that the sample

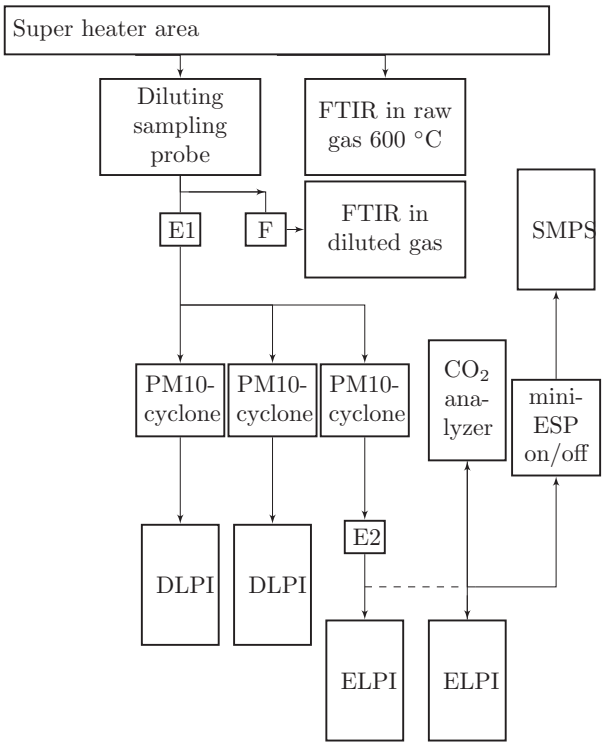

Fig. 1. Measurement setup. E is ejector type diluter, F is a particle filter, and PM10-cyclone is a cyclone with 10 µm cut–off diameter. The diluted sample was taken at 900–1000 °C temperature area and the raw flue gas sample at 600 °C temperature area of the boiler. The dashed line indicates the 11-m long sampling line.

cools enough in the primary diluter. Primary dilution ratio was changed in one of the experiments to see how sensitive the particle size distribution is to the variations in primary dilution conditions. Secondary dilution was used to lower the temperature of the sample even more to the room temperature. The sample temperature before the secondary diluter was approximately 200 °C.

After the secondary dilution the particles were collected with two parallel Dekati low pressure impactors (DLPI, Dekati Ltd.) in order to measure the mass size distribution and the chemical composition of the particles. A cyclone with cut-off diameter of 10 µm was applied before the DLPIs. The DLPI collection plates were greased polycarbonate films, whereas the smallest particle fraction was collected to a teflon filter. The particulate sample collected by one of the DLPI was used to analyse the water soluble fraction of the particles, and the other to analyse the acid-soluble particles. In this study, 13 size fractions of DLPI were combined afterwards into five different size categories <30 nm, ≥ 30 nm to

Table 2
Fuel properties.

		Industrial pellet	Roasted pellet	Coal
Moisture	%	6.7	6.0	11.0–11.3
Ash	%	0.8	3.3	10.5–11.4
Volatiles	%	78.1	64.6	32.8–33.1
Heating value	GJ/t	17.7	20.3	24.6–24.9
C	%	47.4	53.8	62.3–63.1
H	%	5.6	5.2	4.1–4.2
N	%	0.1	0.3	1.8–2
O	%	39.4	31.7	0
S	mg/kg dry	180	580	3100–4600
Cl	mg/kg dry	39	84.3	236
Ca	mg/kg dry	2300	6100	4300–4800
Mg	mg/kg dry	280	740	1700–1900
Na	mg/kg dry	69	240	1400–1600
K	mg/kg dry	760	3200	2500–2900
Fe	mg/kg dry	140	1100	4800–5700
Al	mg/kg dry	130	580	14200–15000
Ti	mg/kg dry	8.8	47	600–640
Ba	mg/kg dry	26	25	270–280
B	mg/kg dry	<40	<40	210–230
Ag	mg/kg dry	<0.5	<0.5	<0.5
As	mg/kg dry	<0.5	<0.5	4.9–14
Be	mg/kg dry	<0.5	<0.5	<0.5
Bi	mg/kg dry	<0.7	<0.7	<0.7
Cd	mg/kg dry	0.2	1.2	0.1
Co	mg/kg dry	<0.5	<0.5	1.4–2.1
Cr	mg/kg dry	1.2	13	9.7–11
Cu	mg/kg dry	1.6	5.9	7.8–8.5
Li	mg/kg dry	<0.5	1.1	9.3–10
Mn	mg/kg dry	140	140	38-66
Mo	mg/kg dry	<0.5	0.9	1.1–1.3
Ni	mg/kg dry	<0.5	2.3	4.1–6.6
Pb	mg/kg dry	<0.5	6.1	3.4–4.1
Rb	mg/kg dry	2.5	6.4	5.2–9.0
Sb	mg/kg dry	<0.5	<0.5	<0.5
Se	mg/kg dry	<0.7	<0.7	<0.7–1.1
Sr	mg/kg dry	5.5	19	150–170
Th	mg/kg dry	<0.5	<0.5	1.2–1.3
Tl	mg/kg dry	<0.5	<0.5	<0.5
U	mg/kg dry	<0.5	<0.5	<0.5–0.6
V	mg/kg dry	<0.5	1.3	13–15
Zn	mg/kg dry	30	120	11–18

<90 nm, ≥ 90 nm to <260 nm, ≥ 260 nm to <600 nm, ≥ 600 nm to <1.6 μm, and > 1.6 μm.

The water-soluble anion (SO_4^{2-}, Cl^-, F^-) concentrations were determined with ion chromatography (measurement was based on standard SFS-EN ISO 10304-1 and instrument that was used was Dionex ICS-2000 Ion Chromatography system). The analysed water-soluble elements were Ca^{2+}, K^+, Na^+, SO_4^{2-}, Cl^-, F^-, and Zn, whereas the acid-soluble fraction was analysed for 31 elements (Ag, Al, As, B, Ba, Be, Bi, Ca, Cd, Co, Cr, Cu, Fe, K, Li, Mg, Mn, Mo, Na, Ni, Pb, Rb, Sb, Se, Sr, Th, Ti, Tl, U, V, Zn, Cl and S). Elements (water-soluble cations and acid-soluble elements) were determined with an Induction Coupled Plasmonic – Mass Spectrometer (ICP-MS). Measurement was based on standard SFS-EN ISO 17294-2 and the instrument that was used was a Thermo Fisher Scientific iCAP Q ICP-MS. It has to be noted that Si, carbon, carbonates and oxides were not analysed from the samples. The water-soluble cations and anions were dissolved in 25 ml of ultra-pure Milli-Q water in closed plastic tubes at room temperature for 5 days. During the dissolution, the samples were shaken for 2 h and stored for 2 h in an ultrasound bath. The acid-soluble elements were dissolved in 2 ml of nitrous acid–hydrogenfluoride acid (3:1) solution and the sample was diluted with 10 ml of Milli-Q water.

After the secondary dilution, part of the sample was diluted further with dilution ratio of 12 and conducted to an Electrical low-pressure impactor (ELPI, Dekati Ltd., Keskinen et al. [25]). ELPI was used parallel with the DLPIs to monitor the loading of the collection plates of DLPIs. Further, part of the sample flow was led with an 11-m-long sampling line to a scanning mobility particle sizer (SMPS, Wang and Flagan [26]), another ELPI and a CO_2 analyser (SickMaihak, SIDOR). These instruments were installed inside an air-conditioned room. The SMPS consisted of DMA 3071 (TSI Ltd.) and CPC 3025 (TSI Ltd.) with 0.6/6.0 lpm flows a thus corresponding to particle size range from 9.8 nm to 414 nm. The charging state of the particles was studied by utilizing a self-made electrostatic precipitator (mini-ESP). The mini-ESP was used in part of the measurements to remove the electrically charged particle fraction before the SMPS size distribution measurement. A schematic of the measurement setup is presented in Fig. 1. The diffusional losses for particles in the 11-m sampling line were calculated (Hinds [27, Eqs. (7-31) and (7-32)]) to be for 10 nm, 20 nm, 40 nm and 100 nm particles in diameter 48%, 25%, 10%, and 4%, respectively. The particle size distributions below have been corrected by these values.

In addition to particle measurements, the concentrations of gaseous species were measured simultaneously after primary dilution from the same sampling line as the particles. Gaseous components were measured with an FTIR gas analyser (Gasmet DX-4000), in which the optical path was 5.0 m. The gaseous sam-

Table 3
Concentrations of gaseous compounds CO_2 (% red. dry 6% O_2, marked as % r.) and CO, NO, SO_2, HCl, HF (ppm reduced dry 6% O_2, marked as ppm r.), total particle number concentration (N_{tot}, calculated from particle number size distribution measured with SMPS) and PM10 in the wet flue gas boiler reheater area. The "c" corresponds to coal and "rp" to roasted pellet and "ip" to industrial pellet; the percentages are the amount of pellet thermal power of the total fuel power.

Fuel	CO_2 (% r.)	CO (ppm r.)	NO (ppm r.)	SO_2 (ppm r.)	HCl (ppm r.)	HF (ppm r.)	N_{tot} ($\cdot 10^8$ cm^{-3})	PM10 $mgNm^{-3}$
c	13± 0.2	19.5± 2.3	289± 8.4	204± 13	18± 1.3	33.2± 0.8	2.76	600
c+rp6.8%	13± 0.2	18.3± 3.1	276± 23.5	158± 17.3	9± 1.1	29.3± 1.5	2.03	690
c+rp7.6%	13± 0.2	13.6± 1.1	272± 9.6	156± 14.6	9± 0.5	32.3± 1.6	1.90	510
c+rp9.8%	13± 0.2	11.9± 2.3	273± 16.7	183± 10.4	8± 0.4	32.1± 0.8	1.67	720
c+rp13.1%	14± 0.3	12.7± 3.6	294± 27.6	144± 10.4	14± 1	29.7± 0.8	1.73	820
c+ip6.6%	14± 0.2	16.0± 0.9	295± 16.9	146± 5.6	11± 0.7	30.5± 0.7	1.89	640
c+ip10.5%	14± 0.2	18.5± 1.6	278± 11.8	201± 6.1	16± 0.4	30.9± 0.7	2.20	570

ple was kept at 180 °C temperature. The gaseous components were also measured after the reheater where the flue gas temperature was around 600 °C. The measurement place was chosen to be at the reheater area due to lack of viewports at the superheater area. FTIR gas analyser (Gasmet DX-4000) was also used here, with the optical path of 2.5 m. The gaseous sample was taken with sampling probe made by M&C. This FTIR included also a zirconium oxide sensor to measure the humid sample gas oxygen content. The measured gaseous components were H_2O, CO_2, CO, N_2, NO, NO_2, SO_2, HCl, and HF.

The flue gas particles of one coal–pellet mixture "c+ip10.5%" were collected with a flow-through-type sampler onto holey carbon grids for microscopy studies. These particle samples were studied later with a transmission electron microscope (TEM, Jeol JEM-2010) equipped with energy dispersive X-ray spectrometer (EDS, Noran Vantage with Si(Li) detector, Thermo Scientific).

3. Results

3.1. Gaseous compounds

Table 3 shows the gaseous compounds (CO_2, CO, NO, SO_2, HCl and HF) studied from the boiler reheater area. Within the accuracy of measurements, no significant differences in the CO_2 concentration was observed. Concentration of carbon monoxide was lower for pellet–coal mixtures than for coal. The lowest CO concentration was achieved with "c+rp9.8%" (11.9 ppm) and the highest with coal (19.5 ppm). There was hardly any NO_2 present at the flue gas (<2 ppm) and, thus, the NO_x consisted mainly of NO. It can be seen that the pellet addition also decreased the SO_2, HCl and, in some cases the NO concentrations when compared to coal combustion. In principle the reductions of SO_2 and HCl concentrations were presumable due to the chemical composition of the fuels; pellets contain less sulphur and chloride compared to coal. However, the decrease in SO_2 concentration can be affected by changes of combustion and flue-gas processes such as conversion of SO_2 to SO_3 that may promote the existence of sulphate in particle phase. Lower carbon monoxide concentrations with pellet–coal mixtures can be due to higher oxygen content of the fuel.

3.2. Particle mass size distribution and chemical composition

Particle mass on each DLPI stage was weighted in order to gain the particle mass size distribution which is shown in Fig. 2. The particulate mass (below 10 µm, PM10) was calculated from the size fractioned masses and the PM10 was averaged between the two parallel particle collections. The PM10 values were 600 $mgNm^{-3}$, 690 $mgNm^{-3}$, 510 $mgNm^{-3}$, 720 $mgNm^{-3}$, 820 $mgNm^{-3}$, 640 $mgNm^{-3}$ and 570 $mgNm^{-3}$, respectively for

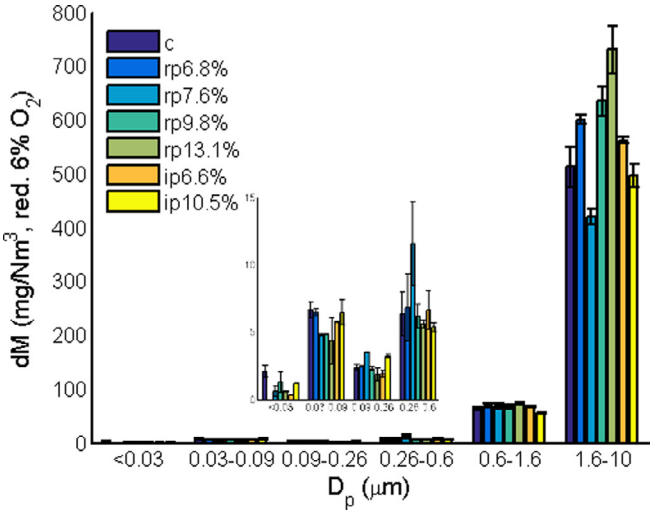

Fig. 2. Particle mass size distribution ($mgNm^{-3}$) calculated from the weighted particle samples that were collected with the parallel DLPIs. The bar shows the mean value of the mass on two different impactor stages and the standard deviation is calculated based on the same masses.

"c", "c+rp6.8%", "c+rp7.6%", "c+rp9.8%", "c+rp13.1%", "c+ip6.6%", and "c+ip10.5%" (with the legend in Fig. 2). The PM10 results indicate that the co-combustion of wood pellets and coal does not increase the PM10 in the boiler.

The chemical composition of the particles was determined from the particulate matter collected on the stages of DLPI. Based on the studied chemical components, a maximum of 50% of PM10 could be identified. This means that more than 50–80% of the particles consisted of unanalysed compounds (e.g., Si and black carbon). For instance, Frey et al. reported that, in the emissions of the same power plant, 80% of particle emission were other than water or acid-soluble fraction [28].

The results of size-fractioned ionic and elemental analysis are presented in Appendix C for each fuel mixture. The size fractions were determined based on the D50% diameters of the DLPI. The ionic composition of one size fraction was calculated in two steps: first, all analysed ion concentrations were added up in the specific size range; second, the ratio of the analysed mass of one ion to the whole analysed mass of ions in the specific size was calculated. Similar calculations were made from elemental analysis. The mass of some size fractions was not enough to determine the ionic or elemental composition. Thus, the composition of that kind of size fraction has been left blank in Fig. C.8 of Appendix C. In addition,

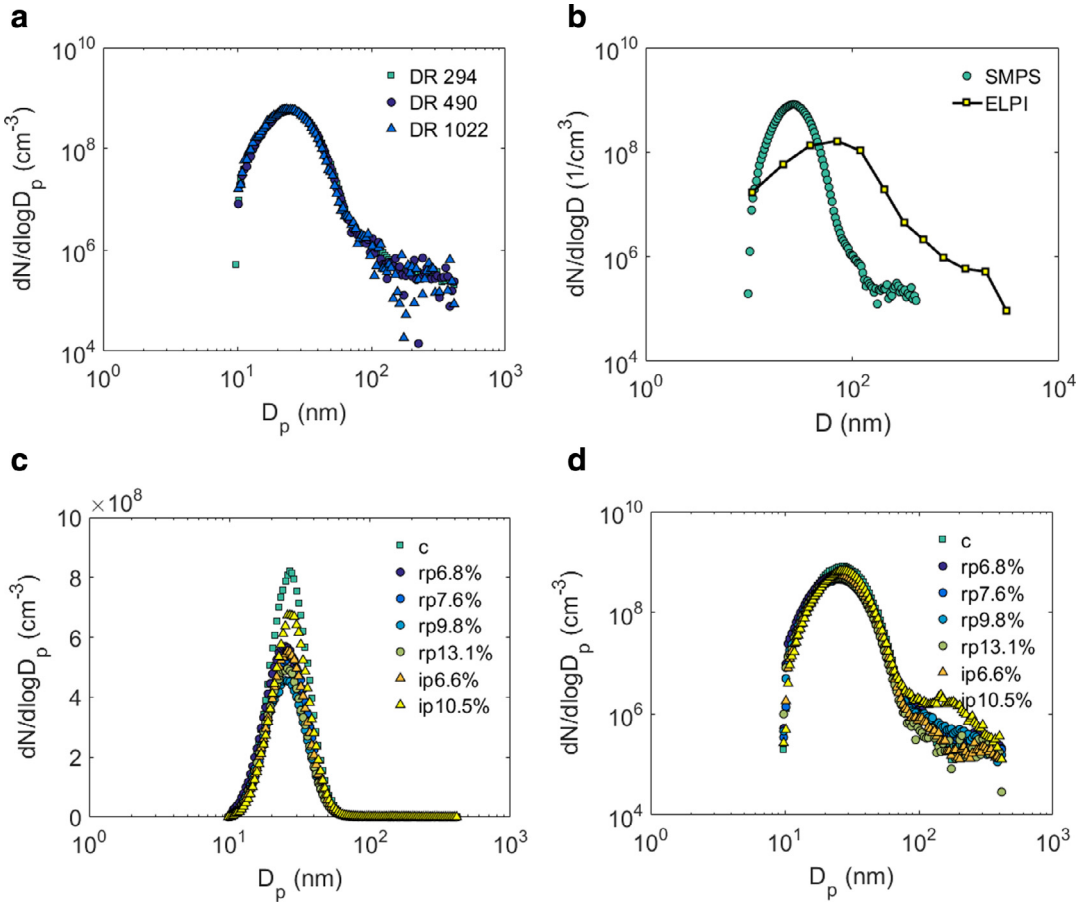

Fig. 3. (a) Effect of total dilution ratio on the measured particle number size distribution (c+rp7.6%). (b) Particle number size distribution measured with ELPI and SMPS (D indicates D_a and D_p in the figure, respectively) during coal combustion. (c, d) Particle number size distributions measured with SMPS. Concentrations have been corrected by the dilution ratio of the whole sampling system.

the missing composition can be due to undetectable concentration of the ions/elements in the sample.

The acid-soluble fraction was 20–50% of the PM10 and the water-soluble fraction was 2–3% of the PM10, specific percentages are shown in Appendix C over the graph. This means that the elemental composition of the particle is more important when studying the chemical composition. For all fuel mixtures, the most common measured elements in the particles were aluminium (Al), calcium (Ca), iron (Fe), magnesium (Mg), potassium (K) and sodium (Na). Aluminium was the main element in particles over 260 nm in diameter, whereas calcium and iron were the most common in particles that were 30–260 nm in diameter. The partition of elements is due to different volatilities of the elements in the fuel [29]. In addition, potassium existed mainly in the particles over 260 nm. The water-soluble fraction consisted mainly of Ca^{2+} and SO_4^{2-} ions in all size classes. In addition to Ca^{2+} and SO_4^{2-}, some K^+ and Na^+ was analysed in the samples. These results indicate that substituting coal with 6–13% of pellets does not have significant effect on the chemical composition of the particles.

3.3. Physical properties of particles

Figure 3a shows the number size distributions of particles (9.8–414 nm) sampled from the boiler super heater area where the temperature was in the range of 900–1000 °C "c+rp7.6%". The geometric-mean diameter (GMD) for the mode dominating the size distributions was around 25 nm. The variation in the dilution ratio did not affect the particle number size distribution corrected by the dilution ratio, which indicates that any of the studied dilution ratios can be used to achieve comparable results [30,31]. It should be noted that in addition to particle concentration, the mean particle size also did not change as a function of the dilution ratio. In other words, there were no significantly low-vapour pressure gaseous compounds that could have formed particles or condensed onto existing particles after the sampling, such as during dilution processes or in other parts of the sampling system. Thus, the results related to the insensitivity of the particle size distribution on the dilution ratio indicate that the particles were formed before the sampling process (i.e., they were present in particle phase already in high temperature conditions).

Figure 3b shows the particle size distribution for coal combustion with two different instruments, namely SMPS and ELPI. The measurement principle of these instruments differs from each other; while the SMPS classifies the particle in respect to their mobility size, the ELPI classifies the particles based on their aerodynamic diameter. The difference between measurement principles enables the evaluation of effective density of particles; see, for example, Ristimäki et al. [32] and Virtanen et al. [33]. Based on the ELPI and SMPS measurements and log-normal-distributions plotted to the size distributions, the particles had a mean mobility diameter of 25 nm and mean aerodynamic diameter of 55 nm. When the effective density is calculated using these particle sizes, its value is 2.05 gcm^{-3}. This is close to the bulk density of SiO_2 which is 2.196–2.648 g cm^{-3}, depending on the crystal form [34]. The effective density of the particles was the same with all studied fuel compositions.

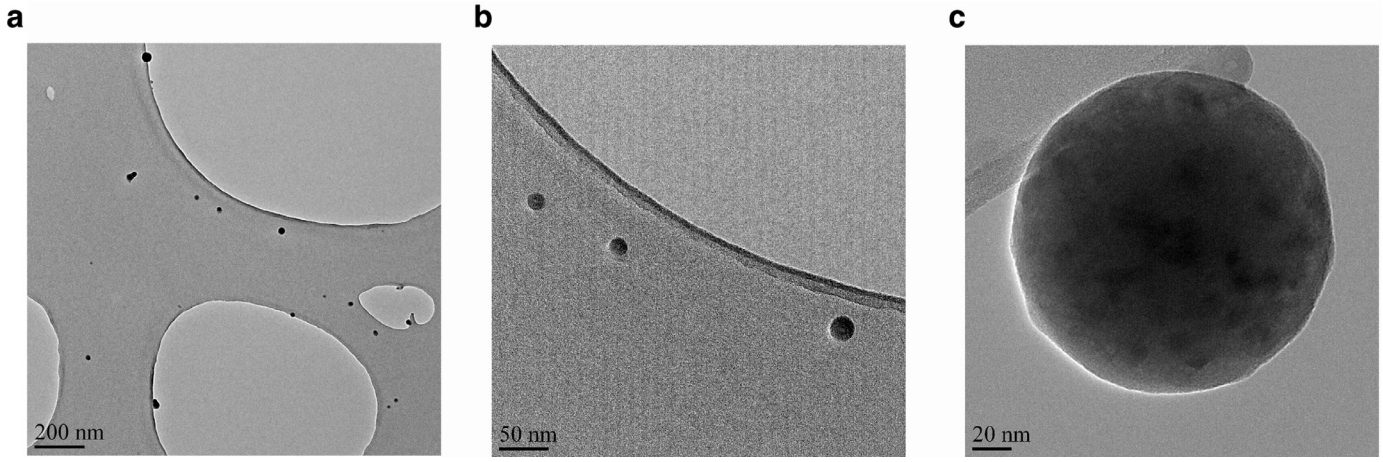

Fig. 4. Transmission electron microscope (TEM) images of particles collected from a flue gas sample. (a) General picture of the small particles, (b) particles having diameters of 10–25 nm and (c) example of larger particle with diameter of 120–130 nm.

Particle number size distribution was dominated by the particles in the range of 10–70 nm in diameter. Figure 3 c shows that the peak concentrations in the number size distribution were not the same with different fuels. The standard deviations for each studied wood pellet–coal mixture are shown in Appendix A. The total particle number concentrations (for particles in the size range of 9.8–414 nm) were calculated from the particle number size distributions and are listed in Table 3. The particle number size distributions were also used to calculate the volume size distribution of the particles (see Appendix B). The 100% coal has the highest peak concentration and, thus, indicates the highest total particle concentration in the boiler super heater area. The second highest peak concentration was observed with coal+ip10.5% case, whereas for the other coal–pellet mixtures total particle concentrations decreased with increasing pellet proportion. However, it seems that also "c+rp13.1%" had an increasing trend to the total particle number concentration (9.8–414 nm) compared with "c+rp9.8%". It can be concluded that the pellet substitution decreases the total particle number concentration in the boiler. The lowest total particle number concentration (9.8–414 nm) was achieved with combustion of roasted pellets and coal because all studied "c+rp"-mixtures, even over 10% substitution, decreased the total particle number concentration equally compared to coal combustion. It seems that over 10% substitution of industrial pellets can actually increase the total particle number concentration in the boiler compared to "c+rp"-mixtures.

Figure 3d shows that the particle number size distributions were mainly unimodal in size range of 9.8–414 nm with a mean electrical mobility diameter of 25 nm and a geometric standard deviation (GSD) of 1.4. However, when combusting "c+ip10.5%"-fuel, the other mode was also observed, in addition to the mode at 25 nm. The other particle mode had the GMD of around 120 nm (GSD 1.6), but the number concentration for this mode was about 3 orders of magnitude smaller than the number concentrations of mode at 25 nm. Thus, the combustion of other "c+rp"-mixtures decreased the total particle number concentration in the studied size range, but did not have an effect on the form of particle number size distribution, and the combustion of "c+ip10.5%" did cause a slightly higher total particle number concentrations and a bimodal particle size distribution. This can be a result of differences in some properties of the fuels, such as the grindability of the pellets. Roasted pellets are more similar to the coal and, thus, could be more easily ground with the coal compared to the industrial pellets which are less processed and look more like stemwood.

The particle sample for transmission electron microscope (TEM) analyses was collected during the combustion of "c+ip10.5%". Examples of the images of the particles are shown in Fig. 4. Based on the images, the typical particle sizes were determined to be 10–25 nm in diameter and 120–130 nm in diameter. Based on the TEM images, particles in both of these size ranges were spherical. The observed diameters correspond well with the particle size distribution measured with the SMPS. Qualitative chemical analysis of the smaller particles, conducted by the EDS method (in Fig. 4b), showed that the particles consisted of Si, Al, P, Fe, Ca and Ti. Similar analysis for larger particles (in Fig. 4c) showed that they consisted of Si, Al, P, Fe, Ca, Ti and Mg. Based on these qualitative analyses, the major difference in the chemical composition of particles was the existence of magnesium in larger particles.

The SMPS measurement for the aerosol sample (Fig. 3c and d) produced a number size distribution of all particles in the size range of the instrument. However, by using the mini-ESP upstream of the SMPS, the measurement produced the number size distribution of electrically neutral particles (i.e., electrically charged particles were removed from the sample before the size distribution measurement). The fraction of electrically charged particles was then calculated by subtracting the concentrations of electrically neutral particles from the concentrations of all particles. This was made for the particle size range of 20–80 nm in which range the particle concentrations were relatively high.

In addition to the results calculated from the measurements, the theoretical charging probabilities were calculated with two different charging probability functions: Boltzmann equilibrium charge distribution [35] and Wiedensohler parametrization [36]. Boltzmann equilibrium charge distribution was calculated in four different temperatures (293 K, 773 K, 1073 K and 1373 K), assuming 1–6 elemental charges of both polarities. The Boltzmann charging probabilities are shown in Fig. 5 with labels "B". Figure 5 also includes the charging probability from Wiedensohler parametrization at room temperature for one elemental charge with both polarities ("W1") and for two elemental charges with both polarities ("W1+W2").

In combustion studies, the amount of electric charge carried by particles have been used as an indicator of the formation temperature of the particles (Maricq [37], Filippo and Maricq [38], Lähde et al. [39], Alanen et al. [40]). In this study, it was observed that the fraction of electrically charged particles in the studied size range was strongly particle size dependent (see Fig. 5), being

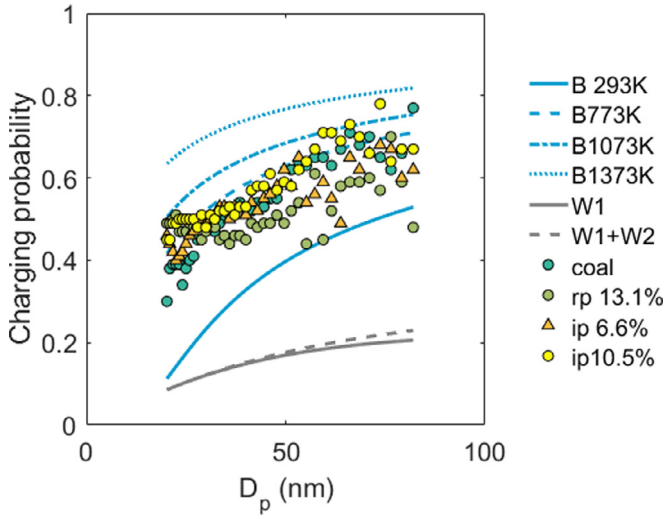

Fig. 5. Fraction of electrically charged particles in the boiler super heater area. Symbols are based on measurement and grey and blue lines denote the charging probability according to Wiedensohler and Boltzmann at different temperatures. (For interpretation of the references to colour in this figure legend, the reader is referred to the web version of this article.)

approximately 40% at 20 nm, 55% at 60 nm and 60% at 80 nm. Due to the mean particle size near 25 nm, for coal combustion, the fraction of electrically charged particles was, on average, 43%. Coal combustion originated particles 20–30 nm in diameter were slightly less charged than the same sized coal-pellet-combustion originated particles. In addition, particles in size range 30–80 nm from "c+rp13.1%" combustion are also less charged than particles from coal or "c+ip" combustion. The charging probability calculated based on particle size distribution measurements was higher than the charging probabilities calculated from Wiedensohler parametrization. This result is thought to be expected because the Wiedensohler parametrization is valid only at room temperatures. Actually, the comparison of measurement results with Wiedensohler parametrization indicates that the particles carried three to four times more electrical charge than the particles formed at room temperature.

When we took into account 1–4 elemental charges in one particle and calculated the Boltzmann charging probability, the charging probability at room temperature was similar to the Wiedensohler parametrization for the 20-nm particles in diameter, but closer the measurement results for the 80-nm particles in diameter. However, when the Boltzmann charging probability was calculated at elevated temperatures, the charging probability was approaching the charging probability that was calculated based on the measurements. The best fit between the Boltzmann charging probability and experimental results was gained at approximately 800 K. This similarity in charging probabilities at 800 K indicates that the particles have been formed at high temperatures. However, it has to be kept in mind that the Boltzmann temperature, at particle sizes below 50 nm in diameter, must be interpreted cautiously. It is also known from the measurements that the sample temperature after primary dilution was approximately 200 °C, which is less than the temperature predicted by the Boltzmann charging probability. This strongly supports the interpretation above (related to the insensitivity of particle size distribution on primary dilution ratio) that the particles were formed in the boiler before the primary dilution process of the sample.

4. Discussion

Fuel choices affect the aerosols released in combustion in power plants. The results of this study showed that coal–pellet mixture combustion reduces SO_2 concentrations in flue gas in comparison with pure coal combustion, which is reasonable based on the chemical composition on the fuels. In addition, coal–pellet mixture combustion reduced the concentrations of CO, and HCl concentrations so that the combustion was cleaner than the combustion of coal alone. Decrease of CO concentrations may be caused for example by the oxygen content of pellet fuels or changes of processes in combustion and flue gas. Additional reasons for the decrease in CO concentration could be the fuel particle size distribution, increased amount of volatile matter, but also using wood and, thus, improving the ignition of coal [41]. However, our data set does not offer unambiguous explanation for the decreased CO concentration. CO_2 concentrations of the flue gas did not change significantly because of fuel changes. It should be keep in mind that the combustion of pellet–coal mixture reduces indirectly also the CO_2 emissions of the power plant due to the carbon neutrality of the biomass pellets. In order to get information regarding the total benefits from CO_2 perspective e.g., the CO_2 emissions of fuel transportation should be taken into account.

In this study, the chemical composition of the particles sampled from the super heater area was very similar to all studied fuel combinations and, thus, it can be concluded that the 6–13% pellet substitution may not increase the corrosion risk of the boiler or super heaters. Nonetheless, the corrosion of boiler and super heater surfaces is a complicated process affected by both the initially gaseous and particulate compounds, as well as the temperature conditions in the boiler, and the detailed understanding of how the fuel changes affect those requires more detailed studies.

Combustion aerosol particles have been previously studied in power plants mostly by measurements for the flue gas in the stack or in duct before ESP. In this study, the particles were studied from the super heater area of the power plant. In general, the results are in line with previous studies made at the stack [42–45]. The results indicated that fuel changes have not had major effects on particle mass and the number size distributions of the flue gas. In addition, results show very clearly that, with all fuel mixtures studied here, the particle number size distributions (from 9.8 nm to 414 nm) were dominated by nanoparticles with a mean size of approximately 25 nm. From the emission point of view, this particle size is problematic because, in general, electrical charging of nanoparticles is not as efficient as the charging larger particles. For example, Ylätalo et al. [46] have shown that sub-100 nm particles penetrate through ESP. Thus, removal of these particles from the flue gas may require techniques other than electrostatic precipitators (ESP). Compared to the combustion of coal only, the combustion of coal–pellet mixtures was observed to decrease the number concentration of nanoparticles and, in addition, slightly increase the fraction of electrically charged nanoparticles. If the power plant is equipped with ESPs, both of these effects have the potential to decrease the particle emissions into the atmosphere. Thus, from the viewpoint of flue gas cleaning and particle emissions, the possible effects of co-combustion of coal and biomass pellets seems to be more positive than negative.

The particle number size distribution measurements supported by other measurements indicated that, for all fuel mixtures, the particles were solid, chemically stable and a significant part of them was electrically charged. For one fuel mixture (over 10% substitution of coal with industrial pellets), the particle number size distribution was observed to consist of two modes, and according to TEM analyses, both of these modes consisted of spherical particles. In general, although the particle measurements were made after diluting the flue gas sample and thus decreasing

its temperature into the room temperature, the results strongly indicate that the measured particles were formed at high temperature conditions before the sampling and dilution process. In addition to the chemical composition of the particles, this was also indicated by the insensitivity of the particle size distribution (number and size of particles) on the primary dilution ratio, as well as by the observation that the measured particles carried electric charge typical for high-temperature aerosol. Overall, the fraction of neutral/charged particles is at the same level as previously reported by Maricq [37] for particles originating from gasoline and diesel engines (data followed Boltzmann charge distributions at 800–1100 K). Thus, the measurement (sampling, dilution, instrumentation) setup used in this study is suitable to get information on particles existing in the high-temperature flue gas. On the other hand, results indicate indirectly that the flue gas from coal combustion and from the combustion of coal–pellet mixtures do not include a lot of such gaseous compounds that can directly condense on particle surfaces.

5. Conclusions

The transition from fossil fuel combustion to biomass combustion has been started, although relevant policies to support this transition are not yet in place. This study characterized how the substitution of coal with pellets changes the flue gas composition in the power plant super heater area. Gaseous components in the flue gas are directly affected by the fuel chemical composition; for example, the concentration of SO_2 and HCl were decreased in the flue gas by pellet substitution. The fuel oxygen content may improve the combustion which can be detected as lower CO concentration in the flue gas.

In addition to changes in the gaseous compounds of the flue gas, the particle chemical and physical properties might also be affected by the fuel changes. In this study, it was detected that the particle mass size distribution did not change significantly between the studied pellet–coal mixtures. However, the PM10 varied between 510 and 820 mg $N\,m^{-3}$. The particle samples gained from the determination of the particle mass size distribution were further analysed. The elemental and ionic analysis showed that the chemical composition of the particles was quite similar which indicates that the pellet–coal mixtures in 6–13% does not increase the corrosion risk. Even though the particle mass size distributions were similar with all of the fuels that were studied, the particle number size distributions have some differences, meaning that the fuel affects the fine particles in the flue gas. The primary dilution ratio did not have an effect on the particle size distribution, which indicates that the particles are formed before dilution in the boiler. The particle number size distributions have a mean diameter of 25 nm, but with “c+ip10.5%” there is also a second mode at 120 nm in diameter. Although, the second mode has 3 orders of magnitude lower particle number concentration compared to the 1st mode in 25 nm size. The bimodal particle number size distribution and, for “c+ip10.5%”, spherical shape of the particles could be also identified from the TEM images. There was also a difference in the particle number concentration (from 9.8 nm to 414 nm); the coal combustion caused the highest total particle number concentrations ($2.78 \cdot 10^8\,cm^{-3}$) and the “c+rp” the lowest ($1.67 \cdot 10^8\,cm^{-3}$), whereas the flue gas particle number concentrations for the coal–industrial pellet mixture were between these values ($1.89 \cdot 10^8\,cm^{-3}$–$2.20 \cdot 10^8\,cm^{-3}$).

Acknowledgments

The study was conducted in the MMEA WP 4.5.2. of Cleen Ltd., funded by Tekes (the Finnish Funding Agency for Technology and Innovation). Dr. Mari Honkanen is acknowledged for TEM imaging. F.M. acknowledges TUT Graduate School, KAUTE-foundation, TES-foundation for financial support. F.M., P.A. and T.R. acknowledges the financial support from the Academy of Finland (ELTRAN Grant 293437). Juho Kauppinen is acknowledged for performing the boiler sampling and the DLPI sample collections.

Appendix A. Standard deviation for the particle number size distributions

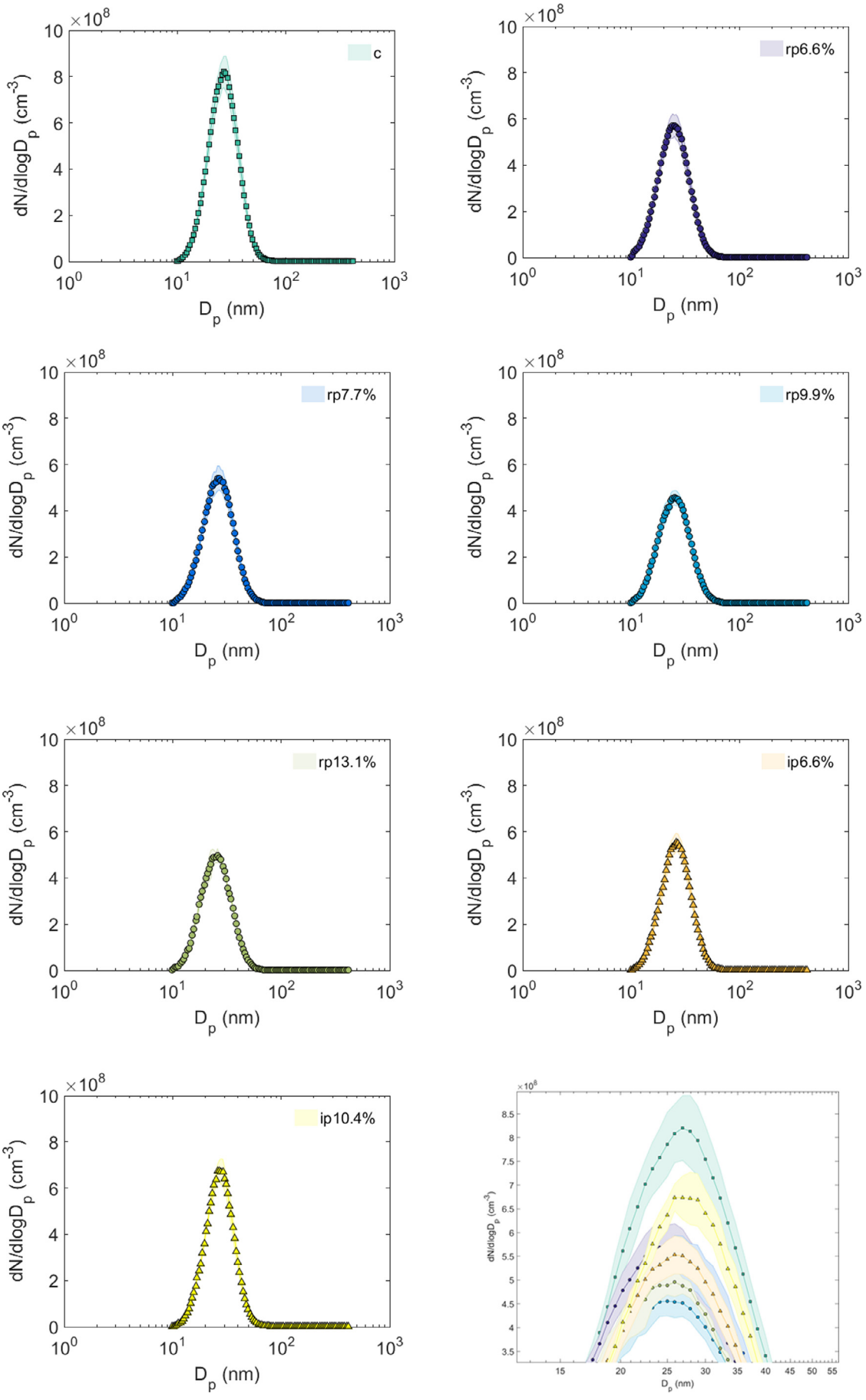

Fig. A.6. Standard deviations of the particle number size distributions measured with SMPS from the boiler super heater area.

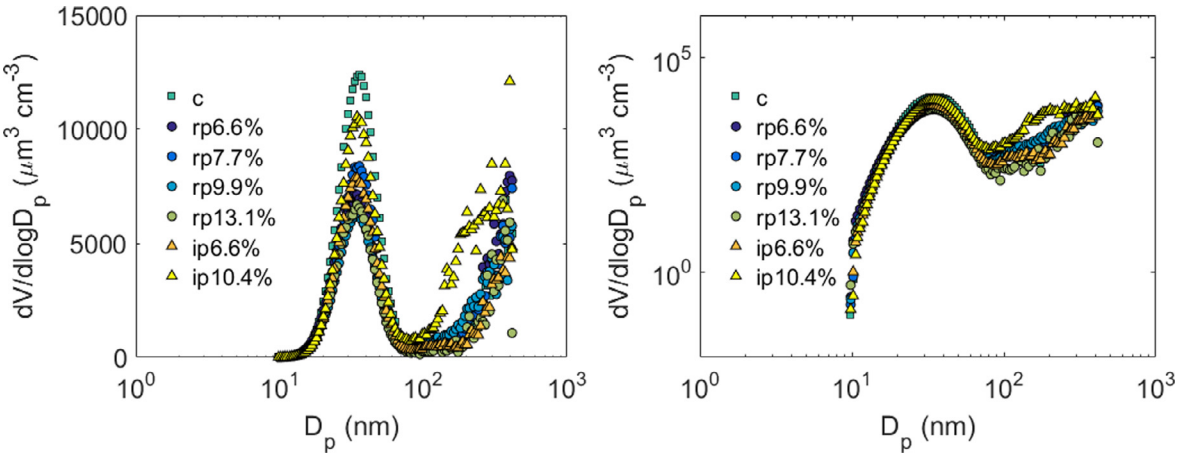

Fig. B.7. Particle volume size distribution calculated based on the assumption of spherical particles from the particle number size distribution measured with the SMPS.

Appendix B. Particle volume size distributions

The mode mean size was 35 nm and for "c+ip10.5%" the second mode mean was 300 nm. The mode mean size cannot be determined for other fuel-mixtures. However, the particle volume size distributions support the mass size distributions shown in Fig. 2.

Appendix C. Particle chemical composition

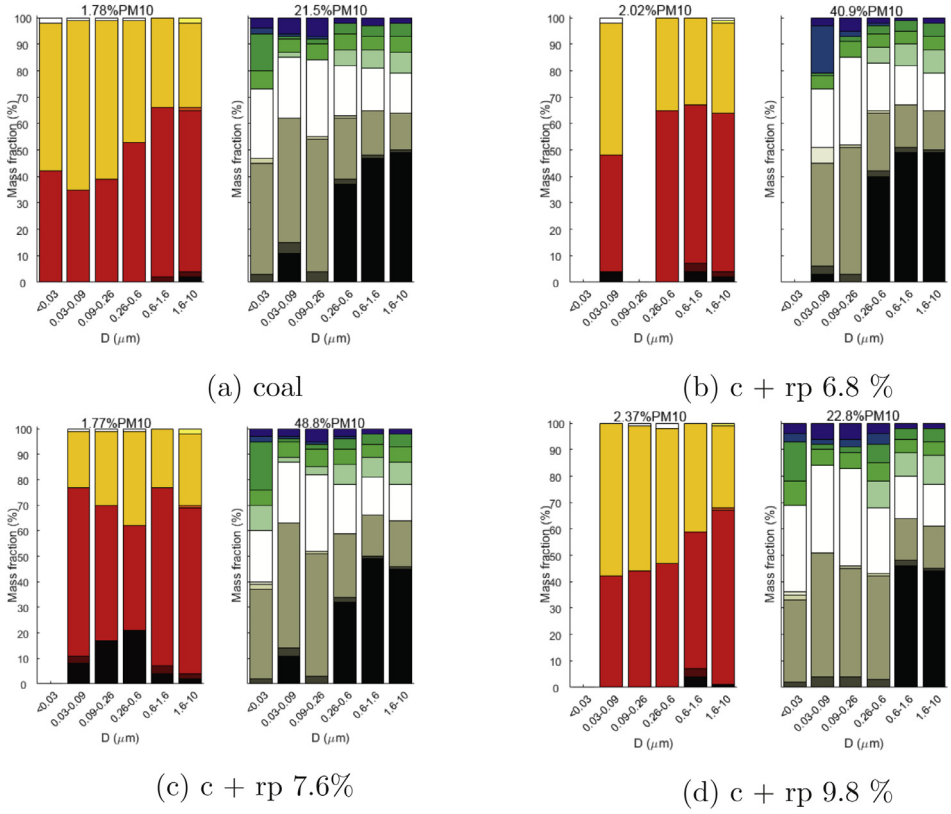

Fig. C.8. Particle chemical composition (ionic on the left and elemental on the right) with joint legend (bottom right) in different coal–pellet mixture cases. The mass ratios are calculated based on total identified mass and, thus some bars only show one chemical component. Studied PM10 mass fractions are presented above each subfigure.

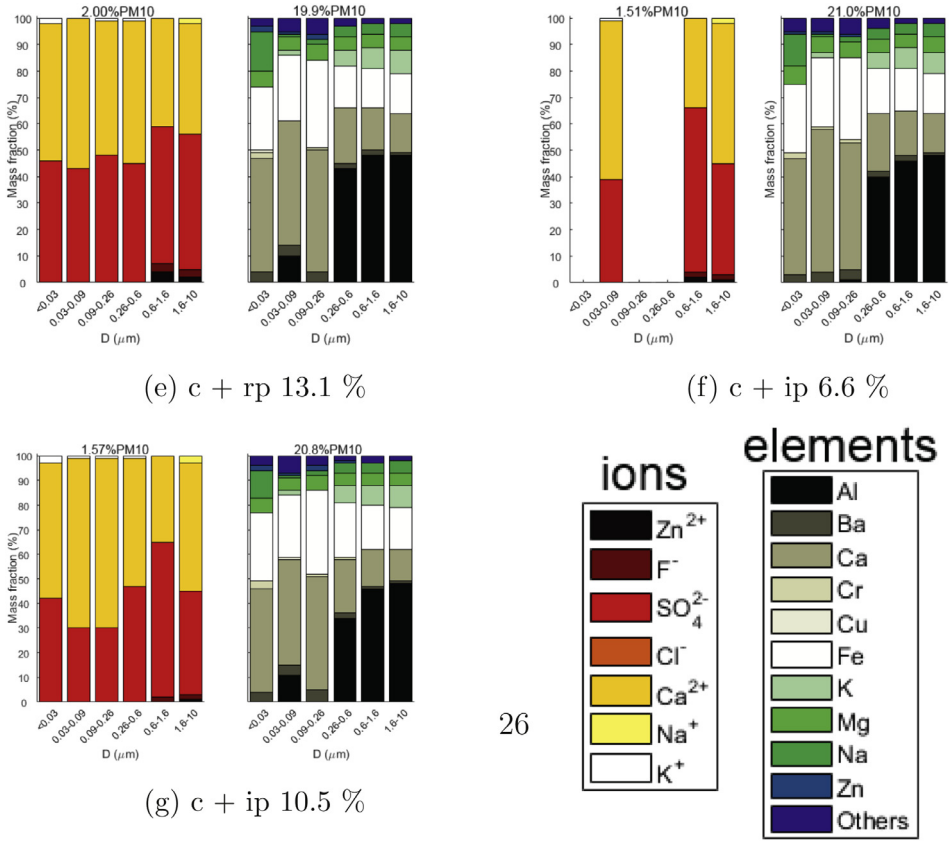

Fig. C.8. Continued

References

[1] U.S., The clean power plan, https://www.whitehouse.gov/climate-change, 2015(accessed 24.11.15).

[2] U.K., 2010 to 2015 government policy: greenhouse gas emissions, https://www.gov.uk/government/publications/2010-to-2015-government-policy-greenhouse-gas-emissions/2010-to-2015-government-policy-greenhouse-gas-emissions, 2015(accessed 24.11.15).

[3] K.V. Shah, M.K. Cieplik, C.I. Betrand, W.L. van de Kamp, H.B. Vuthaluru, Correlatind the effects of ash elements and their association in the fuel matrix with the ash release during pulverized fuel combustion, Fuel Process. Technol. 91 (2010) 531–545, doi:10.1016/j.fuproc.2009.12.016.

[4] B.M. Jenkins, L.L. Baxter, T.R. Miles Jr., T.R. Miles, Combustion properties of biomass, Fuel Process. Technol. 54 (1998) 17–46.

[5] T. Sorvajärvi, N. DeMartini, J. Rossi, J. Toivonen, In situ measurement technique for simultaneous detection of K, KCl, and KOH vapours released during combustion of solid biomass fuel in a single particle reactor, Appl. Spectrosc. 68 (2014) 179–184.

[6] H.P. Nielsen, F.J. Frandsen, K. Dam-Johansen, L.L. Baxter, The implications of chlorine-associated corrosion on the operation of biomass-fired boilers, Prog. Energy Combust. Sci. 26 (2000) 283–298.

[7] H. Kuuluvainen, P. Karjalainen, C.J.E. Bajamundi, J. Maunula, P. Vainikka, J. Roppo, J. Keskinen, T. Rönkkö, Physical properties of aerosol particles measured from a bubbling fluidized bed boiler, Fuel 139 (2015) 144–153.

[8] A. Leppänen, H. Tran, R. Taipale, E. Välimäki, A. Oksanen, Numerical modeling of fine particle and deposit formation in a recovery boiler, Fuel 129 (2014) 45–53, doi:10.1016/j.fuel.2014.03.046.

[9] Y. Ninomiya, L. Zhang, A. Sato, Z. Dong, Influence of coal particle size on particulate matter emission and its chemical species produced during coal combustion, Fuel Process. Technol. 85 (2004) 1065–1088, doi:10.1016/j.fuproc.2003.10.012.

[10] Y. Zhuang, Y.J. Kim, T.G. Lee, P. Biswas, Experimental and theorethical studies of ultra-fine particles behavior in electrostatic precipitators, J. Electrost. 48 (2000) 245–260.

[11] A. Suriyawong, C.J. Hogan, J. Jiang, P. Biswas, Charged fraction and electrostatic collection of ultrafine and submicrometer particles formed during O_2–CO_2 coal combustion, Fuel 87 (6) (2007) 673–682, doi:10.1016/j.fuel.2007.07.024.

[12] United Nations Economic Commission for Europe [UN-ECE], 1999 protocol to abate acidification, eutrophication and ground-level ozone to the convention on long-range transboundary air pollution, as amended on 4 May 2012, ECE/EB. AIR/114, United Nations Economic Commission for Europe [UN-ECE], 6 May 2013.

[13] The European Parliament and the European Council, On the limitation of emissions of certain pollutants into the air from large combustion plants, Directive 2001/80/EC, The European Parliament and the European Council, 23 October 2001.

[14] The European Parliament and the European Council, On industrial emissions (integrated pollution prevention and control) (Recast), Directive 2010/75/EU, The European Parliament and the European Council, 17 December 2010.

[15] The European Parliament and the European Council, On the limitation of emissions of certain pollutants into the air from medium combustion plants, Directive 2015/2193, The European Parliament and the European Council, 28 November 2015.

[16] The European Industrial Bioenergy Initiative, Boosting the contribution of Bioenergy to the EU climate and energy ambitions: implementationplan 2013–2017, Version of 24 January 2014, p. 3. https://setis.ec.europa.eu/system/files/Bioenergy%20EII%202013-2017%20IP.pdf

[17] The European Commission, State of play on the sustainability of solid and gaseous biomass used for electricity, heating and cooling in the EU, SWD(2014) 259 final, The European Commission, Brussels, 28 July 2014, p. 5.

[18] The European Commission, Technology assessment: accompanying the document energy technologies and innovation, COM(2013) 253 final, The European Commission, 2 May 2013, pp. 23, 25.

[19] The European Commission, Impact assessment: accompanying document to the report from the Commission to the Council and the European Parliament on sustainability requirements for the use of solid and gaseous biomass sources in electricity, heating and cooling, COM(2010) 11 final, The European Commission, Brussels, 25 February 2010, pp. 21, 42–43.

[20] National Energy Technology Laboratory, Role of alternative energy sources: pulverized coal and biomass co-firing technology assessment, DOE/NETL-2012/1537, National Energy Technology Laboratory, August 30, 2012, p. VII.

[21] Biomass R&D Board, "The Federal Activities Report on the Bioeconomy", 2016, pp. 34–35. http://www.biomassboard.gov/pdfs/farb_2_18_16.pdf

[22] Environmental Protection Agency, Carbon pollution emission guidelines for existing stationary sources: electric utility generating units; final rule, Fed. Regist. 80 (205) (2015) 64885, 64804(October 23, 2015, Friday).

[23] G. Barbose, Renewables portfolio standards in the united states: a status update, State-Federal RPS Collaborative National Summit on RPS, Washington, D.C., November 6 2013, Environmental Protection Agency (2013), p. 9. https://www.epa.gov/sites/production/files/2015-08/documents/cpp-final-rule.pdf.

[24] M. Aho, P. Vainikka, R. Taipale, P. Yrjas, Effective new chemicals to prevent corrosion due to chlorine in power plant superheaters, Fuel 87 (2008) 647–654. http://dx.doi.org/10.1016/j.fuel.2007.05.033

[25] J. Keskinen, K. Pietarinen, M. Lehtimäki, Electrical low pressure impactor, J. Aerosol Sci. 23 (1992) 353–360.
[26] S.C. Wang, R.C. Flagan, Scanning electrical mobility spectrometer, Aerosol Sci. Technol. 13 (1990) 230–240.
[27] W.C. Hinds, Aerosol technology properties, behavior, and measurement of airborne particles, 2nd ed., John Wiley & Sons, 1999. Eqs. (7-31) and (7-32))
[28] A.K. Frey, K. Saarnio, H. Lamberg, F. Mylläri, P. Karjalainen, K. Teinilä, S. Carbone, J. Tissari, V. Niemelä, A. Häyrinen, J. Rautiainen, J. Kytömäki, P. Artaxo, A. Virkkula, L. Pirjola, T. Rönkkö, J. Keskinen, J. Jokiniemi, R. Hillamo, Optical and chemical characterization if aerosols emitted from coal, heavy and light fuel oil, and small-scale wood combustion, Environ. Sci. Technol. 48 (2014) 827–836.
[29] E.I. Kauppinen, Aerosol formation in coal combustion processes, J. Aerosol Sci. 22 (1991) S451–S454. (Suppl. 1)
[30] U. Mathis, J. Ristimäki, M. Mohr, J. Keskinen, L. Ntziachristos, Z. Samaras, P. Mikkanen, Sampling conditions for the measurement of nucleation mode particles in the exhaust of a diesel vehicle, Aerosol Sci. Technol. 38 (12) (2004) 1149–1160, doi:10.1080/027868290891497.
[31] I. Abdul-Khalek, D. Kittelson, F. Brear, 1999, The influence of dilution conditions on diesel exhaust particle size distribution measurements, SAE Technical Paper 1999-01-1142, SAE, 10.4271/1999-01-1142.
[32] J. Ristimäki, A. Virtanen, M. Marjamäki, A. Rostedt, J. Keskinen, On-line measurement of size distribution and effective density of submicron aerosol particles, J. Aerosol Sci. 33 (11) (2004) 1541–1557.
[33] A. Virtanen, J. Ristimäki, J. Keskinen, Method for measuring effective density and fractal dimension of aerosol agglomerates, Aerosol Sci. Technol. 38 (5) (2004) 437–446.
[34] W.M. Haynes (Ed.), CRC Handbook of Chemistry and Physics, 96th Edition (Internet Version 2015-2016), CRC Press/Taylor & Francis, Boca Raton, FL, 2011, pp. 4–88.
[35] W.C. Hinds, Aerosol technology properties, Behavioir, and Measurement of Airborne Particles, 2nd ed., John Wiley & Sons (1999).
[36] A. Wiedensohler, An approximation of the bipolar charge distribution for particles in the submicron size range, J. Aerosol Sci. 19 (3) (1988) 387–389.
[37] M.M. Maricq, On the electrical charge of motor vehicle exhaust particles, Aerosol Sci. 37 (2006) 858–874.
[38] A.D. Filippo, M.M. Maricq, Diesel nucleation mode particles: semi-volatile or solid? Environ. Sci. Technol. 42 (2008) 7957–7962.
[39] T. Lähde, T. Rönkkö, A. Virtanen, T.J. Schuck, L. Pirjola, K. Hämeri, M. Kulmala, F. Arnold, D. Rothe, J. Keskinen, Heavy duty diesel engine exhaust aerosol particle and ion measurements, Environ. Sci. Technol. 43 (2009) 163–168.
[40] J. Alanen, E. Saukko, K. Lehtoranta, T. Murtonen, H. Timonen, R. Hillamo, P. Karjalainen, H. Kuuluvainen, J. Harra, J. Keskinen, T. Rönkkö, The formation and physical properties of the particle emissions from a natural gas engine, Fuel 162 (2015) 155–161.
[41] A. Gani, K. Morishita, K. Nishikawa, I. Naruse, Characteristics of co-combustion of low-rank coal with biomass, Energy Fuel 19 (2005) 1652–1659.
[42] J. Joutsensaari, E.I. Kauppinen, P. Ahonen, T.M. Lind, S.I. Ylätalo, J.K. Jokiniemi, J. Hautanen, M. Kilpeläinen, Aerosol formation in real scale pulverized coal combustion, J. Aerosol Sci. 23 (1992) S241–S244. (Suppl. 1)
[43] H. Yi, J. Hao, L. Duan, X. Tanf, P. Ning, X. Li, Fine particle and trace element emissions from an anthracite coal-fired power plant equipped with a bag–house in China, Fuel 87 (2008) 2050–2057.
[44] H. Wu, A.J. Pedersen, P. Glarborg, F.J. Frandsen, K. Dam-Johansen, B. Sander, Formation of fine particles in co-combustion of coal and solid recovered fuel in a pulverized coal-fired power station, Proc. Combust. Inst. 33 (2011) 2845–2852.
[45] F. Mylläri, E. Asmi, T. Anttila, E. Saukko, V. Vakkari, L. Pirjola, R. Hillamo, T. Laurila, A. Häyrinen, J. Rautiainen, H. Lihavainen, E. O'Connor, V. Niemelä, J. Keskinen, M.D. Maso, T. Rönkkö, New particle formation in the fresh flue-gas plume from a coal-fired power plant: effect of flue-gas cleaning, Atmos. Chem. Phys. 16 (2016) 1–12.
[46] S.I. Ylätalo, J. Hautanen, Electrostatic precipitator penetration function for pulverized coal combustion, Aerosol Sci. Technol. 29 (1) (1998) 17–30, doi:10.1080/02786829808965547.